

DOI: 10.1002/zaac.202200005



Protonation of Pyruvic Acid – Synthesis of a plain Superelectrophile

Alan Virmani,^[a] Martina Pfeiffer,^[a] Christoph Jessen,^[a] Yvonne Morgenstern,^[a] and Andreas J. Kornath*^[a]

The syntheses of $[\text{H}_3\text{C}(\text{O})\text{CC}(\text{OH})_2][\text{MF}_6]$ and $[\text{H}_3\text{C}(\text{OH})\text{CC}(\text{OH})_2][\text{MF}_6]_2$ ($M = \text{As}, \text{Sb}$) by reacting pyruvic acid in the superacidic systems HF/AsF_5 and HF/SbF_5 are reported. The salts were characterized by low-temperature vibrational spectroscopy and in the cases of $[\text{H}_3\text{C}(\text{O})\text{CC}(\text{OH})_2][\text{SbF}_6]$ and $[\text{H}_3\text{C}(\text{OH})\text{CC}(\text{OH})_2][\text{SbF}_6]_2 \cdot \text{HF}$ by X-ray crystal structure analyses. The exper-

imental results are discussed together with quantum chemical calculations. Remarkably, the bond distance and the twisting angle around the central C–C bond are unaffected by the protonations despite increasing coulombic repulsion. The crystal structure reveals short interionic interactions that have a considerable influence on the C–C bond.

Introduction

The geometry of ethylene dications of the type $[\text{C}_2\text{X}_2\text{Y}_2]^{2+}$ ($X; Y = \text{H}, \text{F}, \text{OH}, \text{NH}_2, \text{SH}$) has been a subject of various theoretical studies as it is the simplest vicinal superelectrophile. It has only been observed in the gas phase.^[1–6] The first study on the potential energy surface of $[\text{C}_2\text{H}_4]^{2+}$ by Schleyer *et al.* suggests a perpendicular structure (D_{2d}) to be most stable with a rotational barrier of 28.1 kcal/mol. This result was explained by hyperconjugation, leading to a significantly shortened C–C bond.^[4] The influence of substituents has been pointed up by Frenking, who found out that ethylene dications containing second-row substituents ($X, Y = \text{F}, \text{OH}, \text{NH}_2$) prefer a planar structure if steric repulsion of adjacent moieties is absent. This is due to π -donation, resulting in a decrease of both the C–C and the C–X distances.^[2] The crystal structures of the chloro and bromo salts of $[\text{C}_2(\text{NMe}_2)_4]^{2+}$, which are obtained by two-electron-oxidation of the neutral ethylene derivative, have a twisting angle of 76° and 67°, respectively. These results by Bock *et al.*^[7] are an attempt of experimental validation of the geometry of ethylene dications, however, the substituents are too big to exclude steric repulsion.

A method other than ionization of neutral ethylene derivatives was established in seminal work by Olah and Prakash, who stabilized a large number of carbocations in superacidic solutions and characterized them mainly by ¹H and ¹³C NMR spectroscopy.^[8–10] Superacids turn out to be a powerful agent to generate and stabilize ethylene dications by protonating non-conjugating π -systems like adjacent carbonyl or carboxyl groups.^[11,12] The same approach was chosen in a recent work, in which the tetrahydroxyethylene dication $[\text{C}_2(\text{OH})_4][\text{SbF}_6]_2$ was obtained by diprotonation of oxalic acid in the superacidic system HF/SbF_5 and the solid-state structure was determined.^[13] Hereby, a planar structure of the dication with two vicinal, carbon-centered positive charges was found. The next step towards the ethylene dication is reducing the number of π -electrons by formally substituting one hydroxy group of $[\text{C}_2(\text{OH})_4]^{2+}$ for a methyl group. Olah *et al.* already generated diprotonated pyruvic acid $[\text{C}_2(\text{OH})_3\text{Me}]^{2+}$ in superacidic solution.^[11] Still, to better understand the geometry of ethylene dications, a structural analysis is yet to be performed. For that, we investigated the behavior of pyruvic acid in the superacidic systems HF/AsF_5 and HF/SbF_5 .

Results and Discussion

Syntheses and properties of $[\text{H}_3\text{C}(\text{O})\text{CC}(\text{OH})_2][\text{MF}_6]$ and $[\text{H}_3\text{C}(\text{OH})\text{CC}(\text{OH})_2][\text{MF}_6]_2$ ($M = \text{As}, \text{Sb}$)

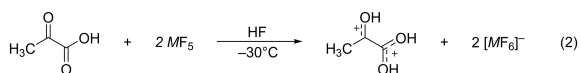
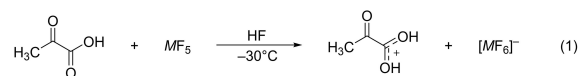
Salts containing the mono- and diprotonated species of pyruvic acid were prepared in the superacidic systems HF/AsF_5 and HF/SbF_5 at -30°C , where anhydrous hydrogen fluoride (aHF) served as both reagent and solvent. Depending on the stoichiometry of the respective Lewis acid, salts of mono- (Equation 1) or diprotonated (Equation 2) pyruvic acid were obtained containing the corresponding anion. The deuterated salts $[\text{H}_3\text{C}(\text{O})\text{CC}(\text{OD})_2][\text{AsF}_6]$ and $[\text{H}_3\text{C}(\text{OD})\text{CC}(\text{OD})_2][\text{AsF}_6]_2$ are generated using anhydrous deuterium fluoride (aDF) as a solvent. Due to the excess of aDF, nearly complete substitution of acidic protons for deuterium is observed.

[a] A. Virmani, M. Pfeiffer, C. Jessen, Y. Morgenstern, Prof. Dr. A. J. Kornath
Department Chemie
Ludwig-Maximilians-Universität München
Butenandtstr. 5–13,
81377 München, Germany
E-mail: andreas.kornath@cup.uni-muenchen.de
Homepage: <http://www.org.chemie.uni-muenchen.de/ac/kornath/>

Supporting information for this article is available on the WWW under <https://doi.org/10.1002/zaac.202200005>

© 2022 The Authors. Zeitschrift für anorganische und allgemeine Chemie published by Wiley-VCH GmbH. This is an open access article under the terms of the Creative Commons Attribution License, which permits use, distribution and reproduction in any medium, provided the original work is properly cited.

All four salts, $[\text{H}_3\text{C}(\text{O})\text{CC}(\text{OH})_2][\text{AsF}_6]$ (1), $[\text{H}_3\text{C}(\text{O})\text{CC}(\text{OH})_2][\text{SbF}_6]$ (2), $[\text{H}_3\text{C}(\text{OH})\text{CC}(\text{OH})_2][\text{AsF}_6]$ (3) and $[\text{H}_3\text{C}(\text{OH})\text{CC}(\text{OH})_2][\text{SbF}_6]$ (4) are soluble in aHF. Isolated, 1 and 2 are stable up to room temperature, 3 and 4 decompose at -28°C . In the case of 2 and 4, colorless crystals grew in aHF at -55°C after 36 h (2) and 72 h (4), respectively. The solvent was then slowly removed at -78°C .



$M = \text{As}, \text{Sb}$

Crystal structure of $[\text{H}_3\text{C}(\text{O})\text{CC}(\text{OH})_2][\text{SbF}_6]$

Monoprotonated pyruvic acid $[\text{H}_3\text{C}(\text{O})\text{CC}(\text{OH})_2][\text{SbF}_6]$ (2) crystallizes in the triclinic space group $P\bar{1}$ with two formula units per unit cell with two symmetrically independent anions. Selected bond lengths, bond angles, dihedral angles, and interionic contacts are listed in Table 1. The cation is displayed in Figure 1.

Table 1. Selected bond lengths, interionic distances [Å], bond angles [deg], and dihedral angles [deg] of 2. Symmetry codes $i = -1 + x, -y, z$; $ii = -1 - x, 1 - y, -z$.

Bond lengths [Å]		Interionic distances D...A [Å]	
C1–C2	1.462(6)	O3...F6ii	2.587(4)
C2–C3	1.541(5)	O2...O1i	2.518(4)
C2–O1	1.211(4)	C3...F1	2.567(5)
C3–O2	1.249(4)		
C3–O3	1.265(5)		
Bond angles [deg]		Dihedral angles [deg]	
C1–C2–C3	118.0(3)	O1–C2–C3–O2	178.8(3)
O3–C3–O2	122.2(4)	C1–C2–C3–O3	177.4(3)
O3–C3–C2	120.5(3)	O1–C2–C3–O3	-2.9(5)
O2–C3–C2	117.3(3)	C1–C2–C3–O2	-0.9(5)
O1–C2–C1	128.1(4)		
O1–C2–C3	113.9(3)		

The crystal packing (Figure S1) and a list of all bond lengths and angles (Table S1) are given in the Supporting Information.

In the cation, the C3–O2 bond is shortened from 1.311(6) Å to 1.249(4) Å, while the C3–O3 bond is elongated from 1.218(6) Å to 1.265(5) Å compared to the starting material.^[14] This is due to π -resonance of the $[\text{C}(\text{OH})_2]^+$ moiety and has been found in various protonated carboxylic acids.^[13,15] Consequently, both CO bonds do not differ significantly. Both the C1–C2 (1.462(6) Å) and the C2–O1 (1.211(4) Å) distances remain approximately unchanged after the protonation. The C2–C3

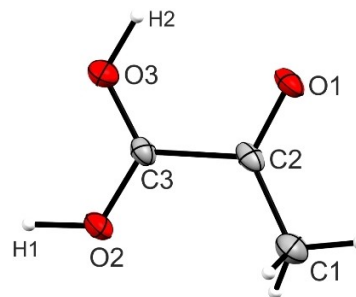


Figure 1. Bare cation $[\text{H}_3\text{C}(\text{O})\text{CC}(\text{OH})_2]^+$ of 2. Probability displacement ellipsoids are set at 50%. Hydrogen atoms are set as spheres of arbitrary radius.

bond length of 1.541(5) Å is only slightly longer compared to the corresponding bond of the starting material (1.529(7) Å).^[14]

As a result of the protonation, the angles O1–C2–C1 and O3–C3–C2 increase whereas the angles O2–C3–C2 and O1–C2–C3 decrease compared to the starting material. The angles C1–C2–C3 and O3–C3–O2 do not change in the course of the protonation. Still, the sums of the respective angles around the C2, and the C3 atom amount to 360° , pointing up sp^2 hybridization of said carbon atoms. The dihedral angle of $2.9(5)^\circ$ remains approximately the same as in pyruvic acid (3.5°).^[14]

The crystal packing shows hydrogen bonds O2...O1i (2.518(4) Å), which connects the individual cations to chains. Two antiparallel chains are linked to each other via an anion, forming O3...F6ii (2.587(4) Å) hydrogen bonds (Figure 2).

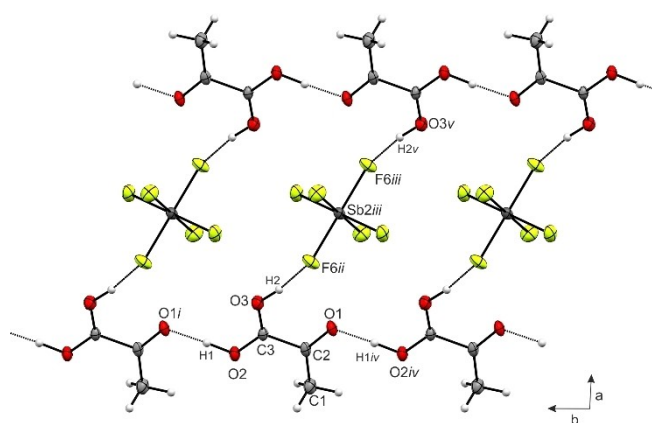


Figure 2. Intermolecular hydrogen bonds (represented as dashed lines) in 2. Symmetry codes $i = -1 + x, -y, z$; $ii = 1 - x, -y, 3 - z$; $iii = x, 1 + y, z$; $iv = 1 + x, y, z$; $v = -1 - x, -1 - y, 3 - z$.

Additionally, a strong, non-hydrogen bridged contact between the carboxylic C3 atom and the F1 atom of the anion is observed (Figure 3). This C3...F1 distance of 2.567(5) Å is approximately 19% below the sum of the van-der-Waals radii

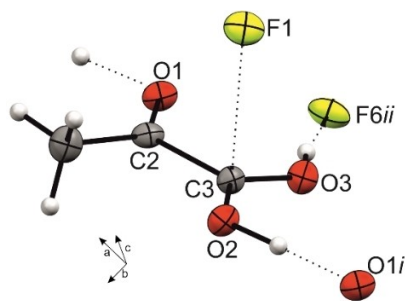


Figure 3. Interionic surroundings of the cation in the crystal packing of **2**. Symmetry codes: $i = -1 + x, y, z$; $ii = -1 - x, -y, 3 - z$.

(3.17 Å),^[16] and the C2–C3...F1 angle adds up to 80.0(2)°. Such interactions are rare but have been reported in literature.^[17]

The antimony atoms Sb1 and Sb2 of the two symmetrically independent anions are located in the inversion centers of the crystal packing. Both anions deviate slightly from the ideal O_h symmetry due to the interionic interactions.

Vibrational spectra of the monoprotonated salts **1** and **2**

Low-temperature infrared and Raman spectra of $[\text{H}_3\text{C}(\text{O})\text{CC}(\text{OH})_2][\text{AsF}_6]$ (**1**), $[\text{H}_3\text{C}(\text{O})\text{CC}(\text{OH})_2][\text{SbF}_6]$ (**2**), and the deuterated species $[\text{H}_3\text{C}(\text{O})\text{CC}(\text{OD})_2][\text{AsF}_6]$ are displayed in Figure 4. For the cation, C_s symmetry and 27 fundamental vibrations, all of which are Raman and IR active, are expected. For the assignment, vibrational frequencies of the geometry-optimized structure of $[\text{H}_3\text{C}(\text{O})\text{CC}(\text{OH})_2]^+$ were calculated at the MP2/aug-cc-pVDZ level of theory. Observed frequencies of pyruvic acid were assigned based on results obtained by Ray *et al.*^[18] A list of selected quantum chemically calculated, and observed frequencies of **1** and **2** are shown in Table 2. The complete assignment is summarized in Table S4.

For the cation, two OH stretching vibrations are expected. In the IR spectra of **1** and **2**, the OH stretching vibrations are superposed by water condensed on the CsBr plate due to our measuring method. Therefore, the OD stretching vibrations of $[\text{H}_3\text{C}(\text{O})\text{CC}(\text{OD})_2][\text{AsF}_6]$ are more meaningful. Those are observed at 2343 cm^{-1} , 2215 cm^{-1} (IR), 2320 cm^{-1} , and 2219 cm^{-1} (Ra).

The out-of-phase CO stretching vibration of the carboxy group of **1** and **2** occurs between 1652 cm^{-1} and 1673 cm^{-1} . The in-phase CO stretching vibration is observed between 1520 cm^{-1} and 1540 cm^{-1} . The corresponding frequencies of the parent compound pyruvic acid are reported at 1771 cm^{-1} (C=O) and 1209 cm^{-1} (C–O).^[18] This observed alignment of the CO frequencies is anticipated due to the protonation. It has to be noted that the carbonylic C=O, as well as the central C–C stretching vibrations of **1** and **2**, remain approximately unchanged.

The frequencies of the anions occur between 186 cm^{-1} and 696 cm^{-1} for the $[\text{AsF}_6]^-$ salt and between 178 cm^{-1} and 670 cm^{-1} for the $[\text{SbF}_6]^-$ salt. For both anions more vibrations are observed than expected for an ideal O_h symmetry,

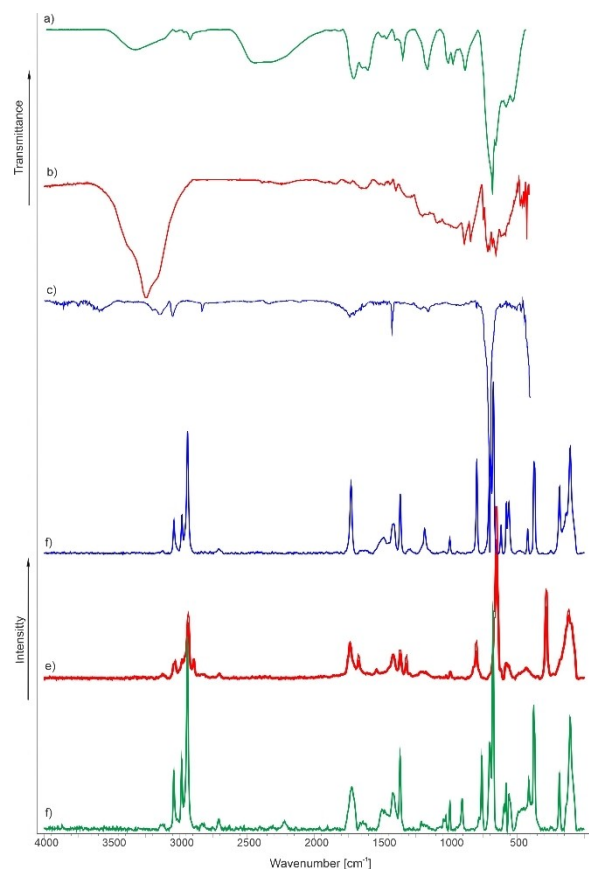


Figure 4. Low-temperature vibrational spectra of $[\text{H}_3\text{C}(\text{O})\text{CC}(\text{O})\text{CC}(\text{OH})_2][\text{AsF}_6]$: a) IR, f) Ra; $[\text{H}_3\text{C}(\text{O})\text{CC}(\text{OH})_2][\text{SbF}_6]$: b) IR, e) Ra; $[\text{H}_3\text{C}(\text{O})\text{CC}(\text{OH})_2][\text{AsF}_6]$: c) IR, d) Ra.

Table 2. Selected observed vibrational frequencies [cm^{-1}] of $[\text{H}_3\text{C}(\text{O})\text{CC}(\text{OH})_2][\text{MF}_6]$ (M = As, Sb) and calculated vibrational frequencies [cm^{-1}] of $[\text{H}_3\text{C}(\text{O})\text{CC}(\text{OH})_2]^+$.

$[\text{C}_3\text{H}_5\text{O}_3][\text{AsF}_6]$ IR	$[\text{C}_3\text{H}_5\text{O}_3][\text{AsF}_6]$ Ra	$[\text{C}_3\text{H}_5\text{O}_3][\text{SbF}_6]$ IR	$[\text{C}_3\text{H}_5\text{O}_3][\text{SbF}_6]$ Ra	$[\text{C}_3\text{H}_5\text{O}_3]^+[\text{a}]$ (IR/Ra)	Assignment
1733	1729	1738	1737	1735 (59/8)	$\nu(\text{CO}_k)$
(vw)	(41)	(vw)	(21)		
1652	1663	1662	1673	1688 (272/1)	$\nu_{\text{oop}}(\text{CO}_a)$
(vw)	(2)	(vw)	(13)		
1520	1526	1523	1540	1557 (144/9)	$\nu_{\text{ip}}(\text{CO}_a)$
(vw)	(1)	(vw)	(6)		
797	797	798 (w)	799	731 (31/10)	$\nu(\text{CC})$
(vw)	(54)		(21)		

[a] Calculated at the MP2/aug-cc-pVDZ level of theory. [b] IR intensities in $\text{km} \cdot \text{mol}^{-1}$ and Raman intensities in $\text{\AA}^4 \cdot \mu^{-1}$. Experimental Raman intensity is scaled to the most intensive mode to be 100. [c] Abbreviations: v = very, w = weak, m = medium, ν = stretch, ip = in-phase, oop = out-of-phase, k = keto, a = acid.

suggesting a distorted octahedral structure. This is confirmed by the X-ray structure analysis for **2**.

Crystal Structure of $[H_3C(OH)CC(OH)_2][SbF_6]_2 \cdot HF$

Diprotonated pyruvic acid $[H_3C(OH)CC(OH)_2][SbF_6]_2 \cdot HF$ (**4**) crystallizes in the triclinic space group $P\bar{1}$ with two formula units per unit cell. Selected bond lengths, interionic contacts, bond angles, and dihedral angles are listed in Table 3. The cation of **4**

Table 3. Selected bond lengths, interionic interactions [Å], bond angles [deg], and dihedral angles [deg] of **4**. Symmetry codes $i = 1 - x, 1 - y, -z$; $ii = 1 - x, -y, -z$; $iii = 1 + x, y, z$.

Bond lengths [Å]		Interionic distances D...A [Å]	
C1–C2	1.451(5)	F13...F3i	2.494(3)
C2–C3	1.526(5)	O3...F12iii	2.554(4)
C2–O1	1.243(4)	O1...F7ii	2.453(4)
C3–O2	1.254(5)	O2...F13	2.492(4)
C3–O3	1.260(4)	C2...F6i	2.598(5)
		C3...F2	2.608(5)
Bond angles [deg]		Dihedral angles [deg]	
C1–C2–C3	119.8(3)	O1–C2–C3–O2	179.6(3)
O3–C3–O2	121.9(4)	C1–C2–C3–O3	–178.6(3)
O3–C3–C2	123.1(3)	O1–C2–C3–O3	–0.2(5)
O2–C3–C2	115.0(3)	C1–C2–C3–O2	1.2(5)
O1–C2–C1	128.1(4)		
O1–C2–C3	112.1(3)		

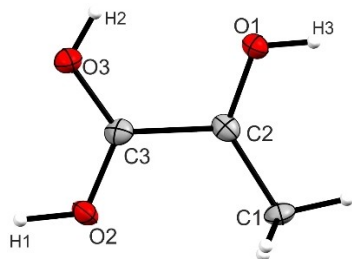


Figure 5. Bare cation $[H_3C(OH)CC(OH)_2]^{2+}$ of **4**. Probability displacement ellipsoids are set at 50%. Hydrogen atoms are set as spheres of arbitrary radius.

is shown in Figure 5. All bond lengths and angles are listed in Table S2. An asymmetrical unit comprising a co-crystallized HF molecule is displayed in Figure S2, the crystal packing in Figure S3.

The C1–C2 bond length (1.451(5) Å) of the cation is in good agreement with known $C(sp^3)–C(sp^2)$ distances,^[19,20] but it is shortened significantly compared to pyruvic acid (1.487(5) Å). The C2–O1 distance of the keto group of pyruvic acid (1.206(6) Å)^[14] is elongated by the protonation to 1.243(4) Å due to π -resonance of the protonated carbonyl group. The CO bond is significantly shorter than in previously reported protonated carbonyl groups,^[21] probably because of the protonated carboxy group as an electron-withdrawing group in the direct vicinity.

The C2–C3 bond distance of 1.526(5) Å is unchanged compared to pyruvic acid (1.529(7) Å)^[14] and **2** (1.541(5) Å). The dihedral angle of 1.2(5)° does not significantly deviate from C_s symmetry. This is rather surprising since no intramolecular hydrogen bonds are observed. Yanai *et al.* found that polarized push-pull ethylene derivatives tend to twist around the C–C bond if the moieties do not interact while increasing the C–C distance significantly.^[22] In our case, the bond length between the two positively polarized C atoms is unchanged relative to the starting material, although coulombic repulsion is present.^[23]

Regarding the bond angles, only the angles O2–C3–C2, which decreases from 117.3(3)° to 115.0(3)°, and O3–C3–C2 that increases from 120.5(3)° to 123.1(3)°, change slightly compared to **2**. The sum of the respective angles around both the carbon atoms amount to 360°, pointing up sp^2 hybridization of the central C atoms.

The cation of **4** exhibits three strong hydrogen bonds to F atoms of two $[SbF_6]^-$ anions (O1...F7ii and O3...F12iii) and one co-crystallized HF molecule (O2...F13) (Figure S4). Interionic interactions are observed between the central C atoms and F atoms of the $[SbF_6]^-$ anion, shown in Figure 6. The distances of

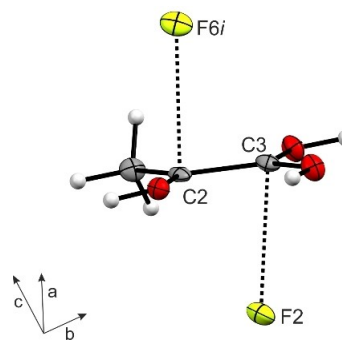


Figure 6. Non-hydrogen bridged C...F contacts in **4**. Symmetry code: $i = 1 + x, y, z$.

C2...F6i (2.598(5) Å) and C3...F2 (2.608(5) Å) are approximately 18% below the sum of the van-der-Waals radii (3.17 Å).^[16] The corresponding angles F6i...C2–C3 (84.4(2)°) and F2...C3–C2 (80.4(2)°) are close to a linear geometry.

Bond lengths of the anions range between 1.853(2) Å and 1.941(2) Å. The distortion of the ideal O_h symmetry is caused by strong interionic interactions.

Vibrational spectra of the diprotonated salts **3** and **4**

Low-temperature infrared and Raman spectra of $[H_3C(OH)CC(OH)_2][AsF_6]_2$ (**3**), $[H_3C(OH)CC(OH)_2][SbF_6]_2$ (**4**) and $[H_3C(OD)CC(OD)_2][AsF_6]_2$ are displayed in Figure 7. Selected observed vibrational frequencies are summarized in Table 4 along with selected calculated values of the cation $[H_3C(OH)CC(OH)_2]^{2+}$ (MP2/aug-cc-pVDZ level of theory). In addition, the quantum

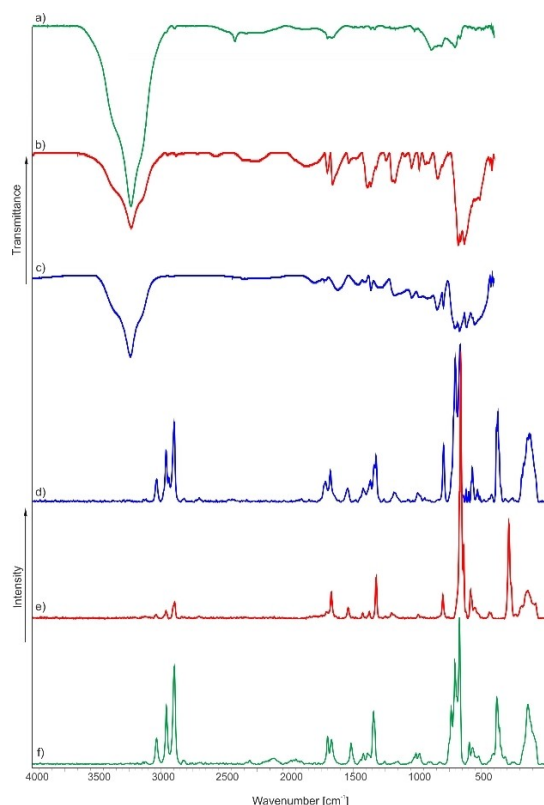


Figure 7. Low-temperature vibrational spectra of $[\text{H}_3\text{C}(\text{OD})\text{CC}(\text{OD})_2][\text{AsF}_6]_2$: a) IR, f) Ra. $[\text{H}_3\text{C}(\text{OH})\text{CC}(\text{OH})_2][\text{SbF}_6]_2$: b) IR, e) Ra; $[\text{H}_3\text{C}(\text{OH})\text{CC}(\text{OH})_2][\text{AsF}_6]_2$: c) IR, d) Ra.

Table 4. Selected observed vibrational frequencies [cm^{-1}] of $[\text{H}_3\text{C}(\text{OH})\text{CC}(\text{OH})_2][\text{MF}_6]_2$ ($\text{M} = \text{As}, \text{Sb}$) and calculated vibrational frequencies [cm^{-1}] of $[\text{H}_3\text{C}(\text{OH})\text{CC}(\text{OH})_2]^{2+}$.

$[\text{C}_3\text{H}_6\text{O}_3][\text{AsF}_6]_2$	$[\text{C}_3\text{H}_6\text{O}_3][\text{SbF}_6]_2$	$[\text{C}_3\text{H}_6\text{O}_3]^{2+}$	Assignment		
IR	Ra	IR/Ra			
1708 (vw)	1717 (13)	1705 (w)	1710 (3)	1731 (172/5)	$\nu_{\text{oop}}(\text{CO}_a)$
	1678 (20)	1662 (m)	1671 (10)	1661 (155/32)	$\nu(\text{CO}_k)$
	1542 (9)	1537 (w)	1540 (4)	1537 (73/14)	$\nu_{\text{ip}}(\text{CO}_a)$
796 (m)	793 (36)	804 (w)	799 (9)	747 (25/7)	$\nu(\text{CC})$

[a] Calculated at the MP2/aug-cc-pVDZ level of theory. [b] IR intensities in $\text{km} \cdot \text{mol}^{-1}$ and Raman intensities in $\text{\AA}^4 \cdot \mu^{-1}$. Experimental Raman intensity is scaled to the most intensive mode to be 100. [c] Abbreviations: v = very, w = weak, m = medium, ν = stretch, ip = in-phase, oop = out-of-phase, k = keto, a = acid.

chemically calculated vibrational modes of $[\text{H}_3\text{C}(\text{OH})\text{CC}(\text{OH})_2]^{2+} \cdot 3 \text{ HF}$ are summarized in Table S9 (Supporting Information). The cation has C_s symmetry and 30 fundamental vibrations, all of which are Raman and IR active. For a complete analysis of the vibrational frequencies, see Table S5 in the Supporting Information.

Due to the poor polarizability of the OH bond, respective stretching modes are not detected in the Raman spectra. In the IR spectra broad bands of water, which condensed on the CsBr plate because of our measuring method, superpose the $\nu(\text{OH})$ vibrations of diprotonated pyruvic acid. The thus more meaningful OD stretching modes are detected in the spectra of $[\text{H}_3\text{C}(\text{OD})\text{CC}(\text{OD})_2][\text{AsF}_6]_2$ at 2343 cm^{-1} and 2120 cm^{-1} in the IR spectrum and 2307 cm^{-1} , 2118 cm^{-1} , and 1949 cm^{-1} in the Raman spectrum.

Regarding the second protonation, the shifts of frequencies of the CO bonds are examined. A blue-shift of the carboxylic $\nu_{\text{oop}}(\text{CO})$ mode of approximately 50 cm^{-1} compared to the monocations is observed, whereas $\nu_{\text{ip}}(\text{CO})$ remains unaffected. The CO stretching mode of the keto group occurs between 1662 cm^{-1} and 1678 cm^{-1} . This indicates a significant red-shift relative to the monoprotonated salts and the parent compound pyruvic acid of between 51 cm^{-1} and 76 cm^{-1} . The stretching vibration of the central C–C bond remains unchanged relative to the monoprotonated species **1** and **2** as well as the starting material.

The frequencies of the anions occur between 128 cm^{-1} and 707 cm^{-1} for the $[\text{AsF}_6]^-$ salt and between 184 cm^{-1} and 681 cm^{-1} for the $[\text{SbF}_6]^-$ salt. For both salts more vibrations are observed than expected for the ideal O_h symmetry of the anion, confirming the distorted octahedral structure shown in the crystal packing of **4**.

Theoretical Studies

Calculations on the naked cations $[\text{H}_3\text{C}(\text{O})\text{CC}(\text{OH})_2]^+$ and $[\text{H}_3\text{C}(\text{OH})\text{CC}(\text{OH})_2]^{2+}$ were carried out at the MP2/aug-cc-pVDZ level of theory. Compared to the data acquired from the X-ray structure analyses, the bond distances are overestimated. To assess the possible influence of adjacent anions on the stability of the carbon scaffold, we performed additional calculations on the MP2/aug-cc-pVTZ level of theory. For that, the optimized structures of the naked dication $[\text{H}_3\text{C}(\text{OH})\text{CC}(\text{OH})_2]^{2+}$ (**A**) and the cation containing five added HF molecules to simulate all adjacent ionic interactions (**D**) as in the crystal structure of **4** were calculated. To quantify the different effects, the cation with three added in-plane HF molecules to simulate hydrogen bonding (**B**) and the cation including two added perpendicular HF molecules to feign C...F interactions (**C**) were also investigated separately. The structures are displayed in Figure 8, the respective bond lengths are listed in Table 5.

The optimized structure of the naked cation **A** overestimates particular bond lengths compared to the X-ray data of **4**. Certain improvements are made when intermolecular interactions are simulated. The C2–O1 distances of the calculated structures containing hydrogen bonds (**B** and **D**) best represent the X-ray structure. Regarding the C2–C3 bond, the calculation of the bare cation considerably overestimates the distance. When simulating all intermolecular interactions as in the crystal structure of **4** (**D**), the best match for the central C–C bond was obtained.

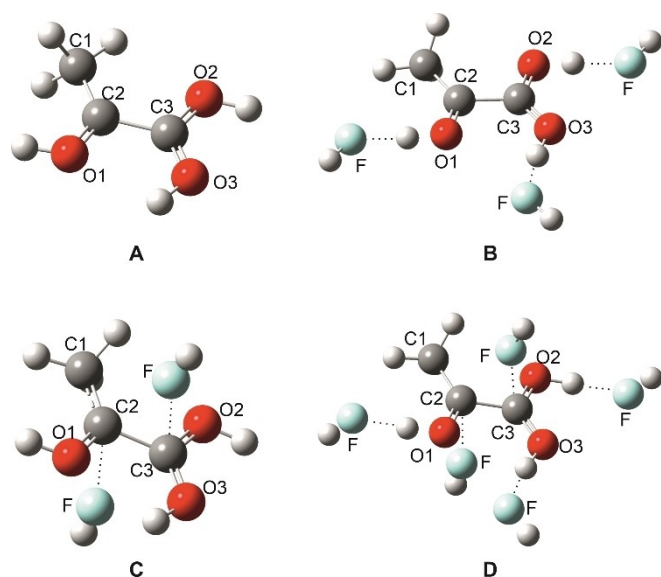


Figure 8. Comparison of the optimized gas-phase structures of $[\text{H}_3\text{C}(\text{OH})\text{CC}(\text{OH})_2]^{2+}$, calculated on the MP2/aug-cc-pVTZ level of theory. Respective interactions are visualized as dashed lines.

Table 5. Comparison of the bond distances [\AA] of the calculated structures A, B, C, and D with X-ray data of 4.

	A ^[a]	B ^[a]	C ^[a]	D ^[a]	X-ray (4)
C1–C2	1.447	1.452	1.445	1.453	1.451(5)
C2–C3	1.548	1.541	1.538	1.534	1.526(5)
C2–O1	1.261	1.251	1.257	1.249	1.243(4)
C3–O2	1.261	1.259	1.262	1.259	1.254(5)
C3–O3	1.263	1.259	1.262	1.259	1.260(4)

[a] Calculated on the MP2/aug-cc-pVTZ level of theory.

All optimizations of the dication reveal C_s symmetry. The C1–C2 bond is shorter than the usual $C(\text{sp}^3)\text{--}C(\text{sp}^2)$ bond.^[20] The hyperconjugation of the methyl group becomes more important if the p-orbital is formally empty. The same conclusion is pulled up in a theoretical study on the ethylene dication to explain the perpendicular D_{2d} structure as the most stable one.^[4] A consistent observation was made by Olah *et al.*, who investigated pyruvic acid in the superacidic system $\text{FSO}_3\text{H}/\text{SbF}_5/\text{SO}_2$ and characterized it by ^1H NMR spectroscopy.^[11] They reported a deshielded singlet methyl absorption at 3.75 ppm. These observations indicate a distribution of the positive charge over both the hydroxy and the methyl group.

Comparing the calculated structures A and B, added in-plane HF molecules lead to a shortening of the C–O bonds, consistent with previous results in our group.^[13,24] Regarding the C2–C3 distance, a slight improvement towards the X-ray data is noted. That means that the strong hydrogen bonds, simulated by HF molecules, facilitate the π -donation of the hydroxy groups into the C(p) orbitals while shortening the C–O distance, similar to the results of a theoretical study on substituted ethylene dications.^[2]

A further stabilizing effect of the C–C bond is found when comparing the naked cation A to the optimized structure with two additional HF molecules to simulate the nearly perpendicular interaction with adjacent anions (C). All bond lengths of A and C are in fair agreement except for the C2–C3 distance, which is in C more similar to the X-ray data than in A, and a better fit than in B, where hydrogen bonds are imitated. This indicates that the greater electron-donating effect into the C(p) orbitals is based on the perpendicular interactions, where the formally unoccupied $p(\pi)$ orbitals receive electron-density from neighboring anions.

These stabilizations are combined in structure D, where the central C–C bond of 1.534 \AA is satisfyingly close to the solid-state structure of 4 (1.526(5) \AA), suggesting that hydrogen bonding and C...F interactions are the main stabilizing effects on the central C–C bond.

Conclusions

In this work, we report the syntheses and isolation of $[\text{H}_3\text{C}(\text{O})\text{CC}(\text{OH})_2][\text{MF}_6]$ and $[\text{H}_3\text{C}(\text{OH})\text{CC}(\text{OH})_2][\text{MF}_6]_2$ by reacting pyruvic acid with MF_5 ($M = \text{As}, \text{Sb}$) in aHF. The compounds were characterized by vibrational spectroscopy and in the cases of the respective $[\text{SbF}_6]^-$ salts by single-crystal X-ray structure analyses. The experimental results are discussed together with quantum chemical calculations. The central C–C bond appears to be unaffected by diprotonation, even though an elongation is expected as former theoretical studies on ethylene dications indicate.^[2,4] In the solid-state, strong hydrogen bonds are observed, facilitating electron donation of the hydroxy groups into the carbon $p(\pi)$ orbitals. Non-hydrogen bridged C...F interactions between a positively charged carbon and a fluorine atom of the anion of nearly perpendicular geometry have an additional significant stabilizing effect on the carbon scaffold.

Experimental Section

Caution! Avoid contact with any of these materials. Hydrogen fluoride will be formed by the hydrolysis of these compounds. HF burns the skin and causes irreparable damage. Safety precautions should be taken when using and handling these materials.

Apparatus and Materials. All reactions were carried out under standard Schlenk conditions by using FEP/PFA reactors closed with a stainless-steel valve and a stainless-steel vacuum line. All vessels were dried with fluorine prior to use. Low-temperature IR measurements were performed with a Bruker Vertex-80 V FTIR spectrometer. A small sample was placed on a CsBr single-crystal plate in a cooled cell. The IR spectra were recorded in a range between 350 cm^{-1} and 4000 cm^{-1} . Raman spectroscopic analysis was performed at -196°C with a Bruker MultiRAM FT-Raman spectrometer with an Nd:YAG laser excitation up to 1000 mW ($\lambda = 1064 \text{ nm}$) in the range between 250 cm^{-1} and 4000 cm^{-1} . Single-crystal X-ray structure investigations were carried out with an Oxford Xcalibur3 diffractometer equipped with a Spellman generator (50 kV, 40 mA) and a KappaCCD detector. The measurements were performed with $\text{Mo-K}\alpha$ radiation ($\lambda = 0.71073 \text{ \AA}$). For data collection, the software CrysAlis CCD^[25] for data reduction the software CrysAlis RED^[26] was used. The solution and refinement

were performed with the programs SHELXT^[27] and SHELXL-97^[28] implemented in the WinGX software package^[29] and checked with the software PLATON.^[30] The absorption correction was achieved with the SCALE3 ABSPACK multi-scan method.^[31] Quantum chemical calculations were performed with the Gaussian 09 program package.^[32] Calculations were carried out employing the method MP2 and the base sets aug-cc-pVDZ and aug-cc-pVTZ. For visualization of the structures and vibrational modes, the program GaussView 5.0^[33] was employed. Pyruvic acid (abcr) was used as purchased, antimony pentafluoride (VWR) was distilled three times prior to use. Arsenic pentafluoride was synthesized from the elements and purified by fractionated distillation.

Syntheses of $[\text{H}_3\text{C}(\text{O})\text{CC}(\text{OX})_2][\text{MF}_6]$ and $[\text{H}_3\text{C}(\text{OX})\text{CC}(\text{OX})_2][\text{MF}_6]_2$ ($\text{X}=\text{H}, \text{D}; \text{M}=\text{As}, \text{Sb}$). For the syntheses of $[\text{H}_3\text{C}(\text{O})\text{CC}(\text{OX})_2][\text{MF}_6]$, first arsenic pentafluoride (170 mg, 1.00 mmol) or antimony pentafluoride (217 mg, 1.00 mmol), respectively, were condensed into a reactor (FEP tube), followed by anhydrous XF ($\text{X}=\text{H}; \text{D}$) at -196°C . Pyruvic acid (88.1 mg, 1.00 mmol) was added under an inert nitrogen atmosphere. The mixture was warmed up to -30°C for 10 min before being cooled down to -78°C again. After removing excess XF in dynamic vacuum overnight, $[\text{H}_3\text{C}(\text{O})\text{CC}(\text{OX})_2][\text{AsF}_6]$ or $[\text{H}_3\text{C}(\text{O})\text{CC}(\text{OX})_2][\text{SbF}_6]$, respectively, were obtained as colorless solids in quantitative yields. The syntheses of $[\text{H}_3\text{C}(\text{OX})\text{CC}(\text{OX})_2][\text{MF}_6]_2$ ($\text{X}=\text{H}, \text{D}; \text{M}=\text{As}, \text{Sb}$) were carried out by using three equivalents of the respective Lewis acid.

Acknowledgments

Financial support of this work by the Ludwig Maximilian University of Munich (LMU), by the Deutsche Forschungsgemeinschaft (DFG) and F-Select GmbH is gratefully acknowledged. Open Access funding enabled and organized by Projekt DEAL.

Conflict of Interest

The authors declare no conflict of interest.

Data Availability Statement

The data that support the findings of this study are available in the supplementary material of this article.

Keywords: superelectrophiles · superacidic systems · X-ray diffraction · vibrational spectroscopy · quantum chemical calculations

- [1] G. Frenking, W. Koch, H. Schwarz, *J. Comput. Chem.* **1986**, *7*, 406.
- [2] G. Frenking, *J. Am. Chem. Soc.* **1991**, *113*, 2476.
- [3] G. Hossein Shafiee, *OJPC* **2012**, *02*, 176.
- [4] K. Lammertsma, M. Barzaghi, G. A. Olah, J. A. Pople, A. J. Kos, P. v R Schleyer, *J. Am. Chem. Soc.* **1983**, *105*, 5252.
- [5] T. Ohwada, K. Shudo, *J. Am. Chem. Soc.* **1989**, *111*, 34.
- [6] G. A. Olah, D. A. Klumpp, *Superelectrophiles and their chemistry*, Wiley, Hoboken, NJ **2008**.

- [7] H. Bock, K. Ruppert, K. Merzweiler, D. Fenske, H. Goesmann, *Angew. Chem.* **1989**, *101*, 1715.
- [8] G. A. Olah, *Angew. Chem. Int. Ed. Engl.* **1973**, *12*, 173.
- [9] G. K. S. Prakash, *Pure Appl. Chem.* **1998**, *70*, 2001.
- [10] G. K. S. Prakash, T. N. Rawdah, G. A. Olah, *Angew. Chem. Int. Ed. Engl.* **1983**, *22*, 390.
- [11] G. A. Olah, A. T. Ku, J. Sommer, *J. Org. Chem.* **1970**, *35*, 2159.
- [12] G. A. Olah, A. M. White, *J. Am. Chem. Soc.* **1967**, *89*, 4752.
- [13] M. Schickinger, T. Saal, F. Zischka, J. Axhausen, K. Stierstorfer, Y. Morgenstern, A. J. Kornath, *ChemistrySelect* **2018**, *3*, 12396.
- [14] K. Harata, N. Sakabe, J. Tanaka, *Acta Crystallogr. Sect. B* **1977**, *33*, 210.
- [15] R. Minkwitz, S. Schneider, M. Seifert, H. Hartl, *Z. Anorg. Allg. Chem.* **1996**, *622*, 1404.
- [16] A. Bondi, *J. Phys. Chem.* **1964**, *68*, 441.
- [17] K. O. Christe, X. Zhang, R. Bau, J. Hegge, G. A. Olah, G. K. S. Prakash, J. A. Sheehy, *J. Am. Chem. Soc.* **2000**, *122*, 481.
- [18] W. J. Ray, J. E. Katon, D. B. Phillips, *J. Mol. Struct.* **1981**, *74*, 75.
- [19] K. Eriks, T. D. Hayden, S. H. Yang, I. Y. Chan, *J. Am. Chem. Soc.* **1983**, *105*, 3940.
- [20] H. Dietrich, *Angew. Chem.* **1961**, *73*, 511.
- [21] D. Stuart, S. D. Wetmore, M. Gerken, *Angew. Chem. Int. Ed. Engl.* **2017**, *56*, 16380.
- [22] H. Yanai, T. Suzuki, F. Kleemiss, H. Fukaya, Y. Dobashi, L. A. Malaspina, S. Grabowsky, T. Matsumoto, *Angew. Chem. Int. Ed. Engl.* **2019**, *58*, 8839.
- [23] D. A. Klumpp, *Chemistry (Weinheim an der Bergstrasse, Germany)* **2008**, *14*, 2004.
- [24] T. Soltner, N. R. Goetz, A. Kornath, *Eur. J. Inorg. Chem.* **2011**, *2011*, 3076.
- [25] CrysAlisCCD, Version 1.171.35.11 (release 16-05-2011 CrysAlis 171.NET), Oxford Diffraction Ltd, UK **2011**.
- [26] CrysAlisRED, Version 1.171.35.11 (release 16-05-2011 CrysAlis 171.NET), Oxford Diffraction Ltd, UK **2011**.
- [27] G. M. Sheldrick, *Acta Crystallogr. Sect. A* **2015**, *71*, 3.
- [28] G. M. Sheldrick, *SHELXL-97, Program for Crystal Structure Solution*, University of Göttingen, Germany **1997**.
- [29] L. J. Farrugia, *J. Appl. Crystallogr.* **1999**, *32*, 837.
- [30] A. L. Spek, *PLATON, A Multipurpose Crystallographic Tool*, Utrecht University, Utrecht, Netherlands **1999**.
- [31] SCALE3 ABSPACK, An Oxford Diffraction Program, Oxford Diffraction Ltd, UK **2005**.
- [32] M. J. Frisch, G. W. Trucks, H. B. Schlegel, G. E. Scuseria, M. A. Robb, J. R. Cheeseman, G. Scalmani, V. Barone, B. Mennucci, G. A. Petersson, H. Nakatsuji, M. Caricato, X. Li, H. P. Hratchian, A. F. Izmaylov, J. Bloino, G. Zheng, J. L. Sonnenberg, M. Hada, M. Ehara, K. Toyota, R. Fukuda, J. Hasegawa, M. Ishida, T. Nakajima, Y. Honda, O. Kitao, H. Nakai, T. Vreven, J. A. Montgomery, J. E. Peralta, F. Ogliaro, M. Bearpark, J. J. Heyd, E. Brothers, K. N. Kudin, V. N. Staroverov, R. Kobayashi, J. Normand, K. Raghavachari, A. Rendell, J. C. Burant, S. S. Iyengar, J. Tomasi, M. Cossi, N. Rega, J. M. Millam, M. Klene, J. E. Knox, J. B. Cross, V. Bakken, C. Adamo, J. Jaramillo, R. Gomperts, R. E. Stratmann, O. Yazyev, A. J. Austin, R. Cammi, C. Pomelli, J. W. Ochterski, R. L. Martin, K. Morokuma, V. G. Zakrzewski, G. A. Voth, P. Salvador, J. J. Dannenberg, S. Dapprich, A. D. Daniels, O. Farkas, J. B. Foresman, J. V. Ortiz, J. Cioslowski, D. J. Fox, *Gaussian09, Revision A.02*, Gaussian, Inc., Wallingford CT **2009**.
- [33] T. K. J. M. R. Dennington, *GaussView, Version 5*, Semichem Inc., Shawnee Mission KS **2009**.

Manuscript received: January 10, 2022

Revised manuscript received: February 6, 2022

Accepted manuscript online: April 26, 2022